Polskie Towarzystwo Materiałów Kompozytowych
Polish Society of Composite Materials

26: 2 (2026) 133–141

COMPOSITES THEORY AND PRACTICE

ISSN (online): 2299-128X

Dariusz Kołacz* (0000-0003-4086-3786), Zbigniew Rdzawski (0000-0001-6667-1972), Joanna Kulasa, Wojciech Głuchowski (0000-0001-9356-9674), Marek Łagoda (0000-0003-3679-6568), Grzegorz Muzia, Krzysztof Wiśniewski (0000-0001-7931-0703), Małgorzata Osadnik (0000-0001-8649-7684)

Lukasiewicz Research Network – Institute of Non-Ferrous Metals, ul. Sowinskiego 5, 44-100 Gliwice, Poland
* *Correspondence*: dariusz.kolacz@imn.lukasiewicz.gov.pl

Received (Otrzymano) 10.05.2026
Published on-line (Opublikowano) 30.06.2026

METHOD OF MANUFACTURING Cu-TiN COMPOSITE MATERIALS

https://doi.org/10.62753/ctp.2026.07.2.2

The article analyses sinters produced by encapsulation and sintering under isostatic pressure (HIP). Copper powders, carbonyl iron powders, and Cu-TiN composite powders were employed in the study, using two chemical compositions: Cu = 98% and TiN = 2% and Cu = 96% and TiN = 4% (wt%). Selected parameters of the encapsulation process and the HIP process parameters used are presented. The apparent density, conductivity, and HBW hardness of the sintered samples were measured, and microstructural studies were performed. High-quality sinters were obtained, with porosity of 0.3% for iron and 0.9% for the Cu(TiN)2 composite.

Keywords: **encapsulation, hot isostatic pressing, metallic powder, composite, sinter, hardness, density, electrical conductivity, microstructure**

INTRODUCTION

The properties of semi-finished products manufactured from copper-based materials are closely linked to their intended use. They also influence the technologies used in their production and processing. In addition to high mechanical properties, materials are typically required to possess sufficiently high electrical and thermal conductivity. Furthermore, when used in components operating at elevated temperatures, these materials must also demonstrate temperature stability.

For this reason, there is a growing trend toward the use of dispersion-hardened copper-based materials. These materials are typically manufactured by powder metallurgy methods, often involving the mechanical synthesis of a copper matrix and a reinforcing phase to achieve nanometric grain sizes. According to previous research, the effect of hardening in materials with nanometric grain sizes is difficult to predict [1]. Some deviations from the Hall-Petch and Orowan relationships are observed, resulting from changes in the deformation mechanism of nanocrystalline materials, the influence of uneven material flow during consolidation and calibration after sintering, related to the presence of grain agglomerates, pores, etc., as well as the effects of solution or precipitation hardening resulting from contamination from abrasive elements of the containers and milling balls, in addition to the heat treatment applied. There is also a risk that during sintering, further hot processing, or the use of these materials at high temperatures, the nanometric structures, and consequently their functional properties, may become unstable. This issue formed the basis for experimental studies of sintering Cu-TiN composite powder under isostatic pressure in the hot isostatic pressing (HIP) process.

Hot isostatic pressing (HIP) is a technological process employed to remove internal porosity in metal castings and other materials [2]. In powder metallurgy, it is utilised to densify powders or mixtures of metallic, ceramic, and composite powders. In the HIP process, the compression medium is an inert gas. The workpiece is simultaneously subjected to high pressure (200 MPa) and a temperature above 2000°C. The HIP process allows high density to be obtained while simultaneously homogenizing the microstructure [3–6]. The HIP process is used, among others, to produce materials for electrical purposes and sinters from alloy powders [7–8]. Powder materials can be densified using the HIP process in two ways. The first involves cold pressing (i.e. cold isostatic pressing) followed by sintering and densification in an HIP press.

In the second method, the powders are sintered in specially designed capsules. A properly prepared powder or powder mixture is enclosed in a metal capsule, which is then placed in the HIP press. The process of encapsulating powder in such capsules is commonly referred to as encapsulation.

The capsules must be tight and deform uniformly under the process conditions. They should be characterised by adequate strength and chemical inertness to chemical reactions that may occur during sintering. Low-carbon steels and stainless steels are often employed as capsule materials. In exceptional cases, titanium or glass is used. Tests utilising glass as a capsule for sintering B4C and Si3N4 compounds have shown that where the shape of the sintered body is highly complex, glass – due to its low viscosity at elevated temperatures – is highly suitable as a container and allows the shape to be reproduced with great accuracy [9–10].

Typically, the wall thickness of capsules ranges from 2 mm to 3 mm. The geometry of the capsule depends on the final product requirements. Changes in the shape of the capsule during the sintering process are influenced by the material and shape of the capsule, the thickness of its walls, the location of the welds, and fluctuations in the density of the powder filling within the capsule.

The simulations confirmed the influence of geometry on the homogeneity of the material after sintering [11]. The method of filling the capsule with powder is also an important issue. Studies have shown that powder compacted in a capsule on a vibrating table may tend to distribute unevenly, and the initial density has a direct impact on the capsule deformation and the final shape of the sinter [12].

The obtained sinters after encapsulation and the HIP process can be subjected to further plastic working, such as the forging of products for special applications. This process aims to shape them and modify their microstructure. Forging leads to intense plastic deformation of the material, resulting in grain refinement. Reducing the grain size increases the strength and hardness of the material, which translates into strengthening. Additionally, the prepared material can be extruded by the KOBO method, which belongs to the group of methods known as severe plastic deformation (SPD). The KOBO process involves simultaneous extrusion of the material and oscillatory rotation of the die, leading to a significant increment in the degree of deformation without the need for high temperatures. This process further refines the microstructure and increases the dislocation density, further strengthening the material [13]. Obtaining a nanometric structure is crucial for the functional properties of the material.

MATERIALS FOR TESTING

Four types of powder samples (wt%) were prepared for comparative sintering tests: Sample 1 = Cu; Sample 2 = Fe; Sample 3 = Cu + 2% TiN; Sample 4 = Cu + 4% TiN. Powders with the following purities (%) were used to prepare the samples: copper – 99.7; titanium nitride – 99.5; and metallic iron – 99.5. Samples 1 and 2 were prepared to verify and select the appropriate conditions for further experiments related to the production of Cu-TiN composites.

Table 1 presents the properties of the powders. The actual density of the studied powders is lower than theoretical one owing to the presence of microporosity in the particles. The specific surface area of the powders is low, below 1 m²/g. Copper powder has an average particle size of approximately d50 = 18 µm, while titanium nitride powder has a slightly smaller particle size of d50 = 6 µm.

TABLE 1. **Properties of powders used for studies and characteristic points of particle size distribution of metallic powders**

Metallic powder	Density, g/cm³	Specific surface area – BET multipoint, m²/g	Characteristic points of particle size distribution (d10, d50, d90)		
			d10	d50	d90
			µm		
Cu	8.86 ± 0.01	0.257 ± 0.007	5.5 ± 0.4	18.5 ± 0.6	45.4 ± 2.3
Fe	7.83 ± 0.01	0.304 ± 0.003	2.6 ± 0.1	6.9 ± 0.2	16.3 ± 0.8
TiN	5.15 ± 0.01	0.967 ± 0.011	1.5 ± 0.1	6.2 ± 0.2	18.8 ± 0.9

Figures 1 and 2 show sample SEM micrographs of the investigated powders. The copper powder particles are characterised by a dendritic shape. The titanium nitride powders have a shape of irregular blocks, while the iron powder particles are spherical in shape.

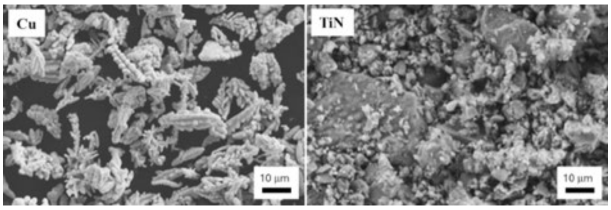

Fig. 1. Sample SEM micrographs of Cu and TiN powders

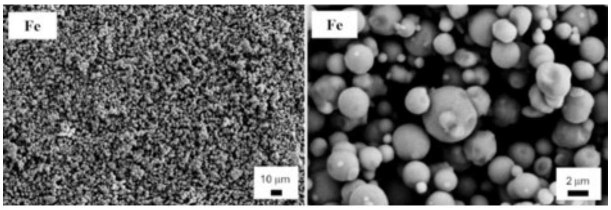

Fig. 2. Sample SEM micrographs of Fe powder

RESEARCH METHODOLOGY

The density of the metal powders was determined using an AccuPyc 1340 device from Micromeritics. The Gemini 2360 device from the same company was utilised to measure the specific surface area. The particle size distribution was measured on a Fritsch NanoTec Analysette 22 by means of the wet laser diffraction method (in water) within a measuring range of 0.10 µm to 504.48 µm, according to Fraunhofer theory.

The mixtures were prepared employing a Turbula-type mixer. The density of the resulting sinters was determined using the Archimedes method. Electrical conductivity was measured by the eddy current method on a Foerster Sigmatest 2.069 instrument. The HBW hardness of 2.5/15.625 was measured utilising a Zwick SuraVision 20 G5 device. The loading time was 20 s. Microstructural studies were performed by means of a Keynce VHX-1 metallographic microscope and a Zeiss Gemini 1525 scanning electron microscope equipped with a Bruker Nano Quantax XFlash 6 X-ray spectrometer.

EXPERIMENTAL STUDIES AND RESEARCH RESULTS

The sintering method used for the metallic copper and iron powders involved encapsulation, hot isostatic pressing (HIP), and mechanical removal of the capsule. In the second case, the process involved mixing in a Turbula-type mixer, encapsulation, sintering, and mechanical removal of the capsule.

The mixing was conducted for 3 h at 45 rpm in the Turbula-type mixer. The prepared mixtures, as well as the metallic powders, were placed in steel containers (capsules) intended for pressure sintering in the HIP process. The capsules were made of 304 and 1.4541 stainless steel. The individual capsule components were joined together using TIG welding. The powder capsule was produced at a station equipped with a CSM-100 encapsulation device from American Isostatic Press Inc. and a loose material compactor.

The sintering process was conducted on an AIP8-30H isostatic press manufactured by American Isostatic Press Inc. Figure 3a shows a view of the CSM-100 device for powder encapsulation in the HIP process and a capsule filled with powder – Figure 3b.

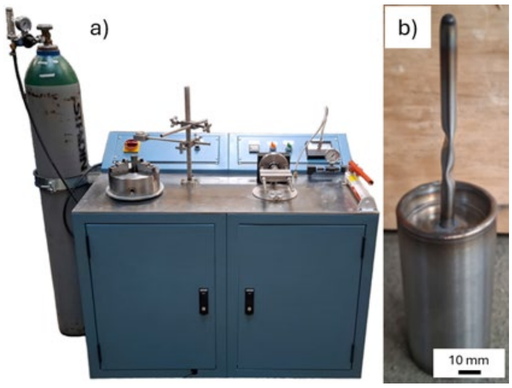

Fig. 3. a) CSM-100 encapsulation device, b) capsule with powder

The encapsulation parameters are presented in Table 2. As previously mentioned, to properly conduct the process, a suitable container – a capsule – was employed. To remove the gas trapped between the loosely packed grains, the powder was compacted utilising a loose material compactor. The process was continued until there was no visible change in the powder volume. For processes 3 to 6, manual compaction was carried out. The compacted powders were tightly sealed in the capsule by means of the TIG material welding process. For processes 3 and 4, a different capsule design was used. The can lids were made from discs and connected with a pipe employing the welding technology.

TABLE 2. **Encapsulation process parameters**

Process no.	Material	Device for loose material compaction		CSM-100 device		
		Use	Comments	Powder degassing process		
				Temp., °C	Time, min	Vacuum, MPa
1	Cu	Yes	-	40	60	$< 1.2 \cdot 10^{-5}$
2	Fe			70		
3	Cu(TiN)2		Mixture was further compacted with a steel stamp	60		
4	Cu(TiN)4					
5	Cu(TiN)2					
6	Cu(TiN)4					

The prepared capsules, containing powders, were placed in an HIP press and sintered under isostatic pressure. The HIP process parameters were as shown in Table 3. After sintering, the capsules were cut open to expose the sinter.

TABLE 3. **HIP process parameters**

Process no.	Material	Temperature	Pressure	Time
		°C	MPa	min
1	Cu	925	100	240
2	Fe	1100	100	180
3	Cu(TiN)2*	950	150	
4	Cu(TiN)4*			
5	Cu(TiN)2	1050	200	120
6	Cu(TiN)4			
*) Cu(TiN)2 means composite Cu + 2 wt% TiN, and Cu(TiN)4 – Cu + 4 wt% TiN				

The density, electrical conductivity, HBW hardness of the sintered samples were measured, and microstructure observations as well as point chemical microanalysis were conducted. Figure 4 shows an example capsule before and after the HIP process, in addition to the resulting iron sinter.

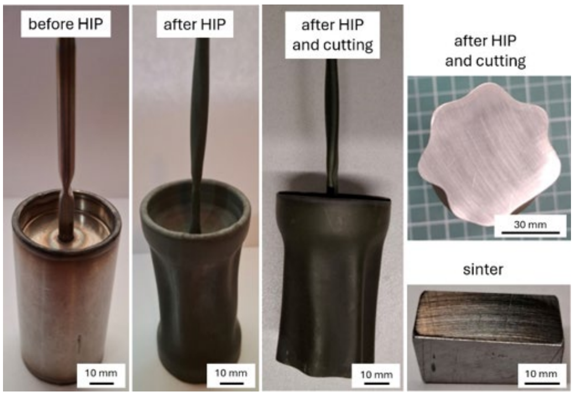

Fig. 4. Capsule before and after HIP process, Fe sinter

Figure 5 illustrates the results of the porosity tests obtained after the HIP process.

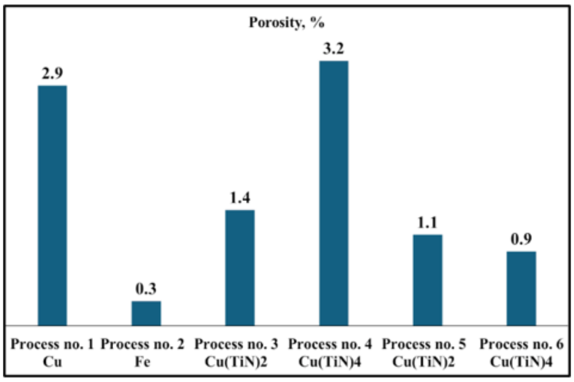

Fig. 5. Porosity of sinters after HIP process

The results of the porosity tests indicate that sinters of satisfactory quality were obtained. The porosity of the sinters made from metallic copper powder, following isostatic pressing at 925°C and 100 MPa for 240 minutes, was 2.9%. In the case of the carbonyl iron sinter, a very high density was achieved (porosity of 0.3%). The use of spherical powder feedstock had a significant impact on the achieved density, resulting in a high bulk density with proper distribution of the powder within the steel capsule. For the Cu-TiN composite sinters, the porosity ranged from 0.9–1.4% for processes 3, 5 and 6, and 3.2% for process 4. Such a sudden increase in porosity (process 4) may have resulted from capsule leakage during the HIP sintering process.

The electrical conductivity for the copper sample was 56.36 MS/m, which is 97% of IACS. In the Cu-TiN composites, it was above 47 MS/m, indicating the formation of a sintered structure and diffusion bonds between the particles – Figure 6.

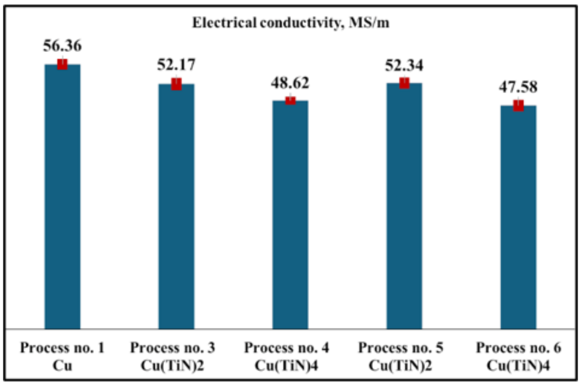

Fig. 6. Electrical conductivity of sinters after HIP process

Figure 7 presents the changes in the hardness of the sinters. The highest hardness 73.1 HBW was obtained for the Fe sinter and the lowest 36.8 HBW for pure copper. The effect of the titanium nitride addition on the strengthening of the Cu-TiN composites was observed. A higher titanium nitride content increased the material hardness.

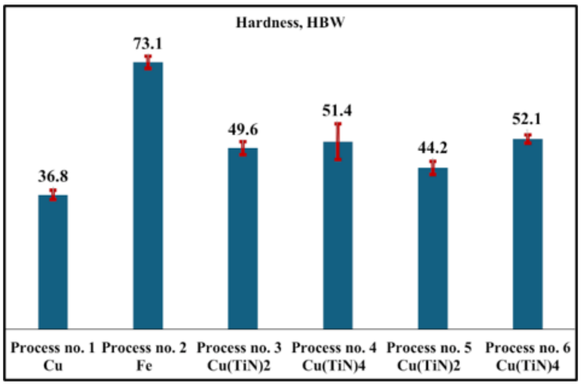

Fig. 7. Hardness HBW of sinters after HIP process

Figures 8a and 8b show cross-sections of the copper (Cu) sinter and the steel capsule, which enabled assessment of the nature of the material bond and the phenomena occurring at the sintered composite–steel capsule interface. Microstructural analysis revealed diffusion of the alloying elements, particularly chromium (Cr) and iron (Fe), from the steel into the copper. The diffusion depth was observed to be approximately 10 µm. The presence of these elements in the copper structure can affect local material properties, such as hardness and electrical conductivity.

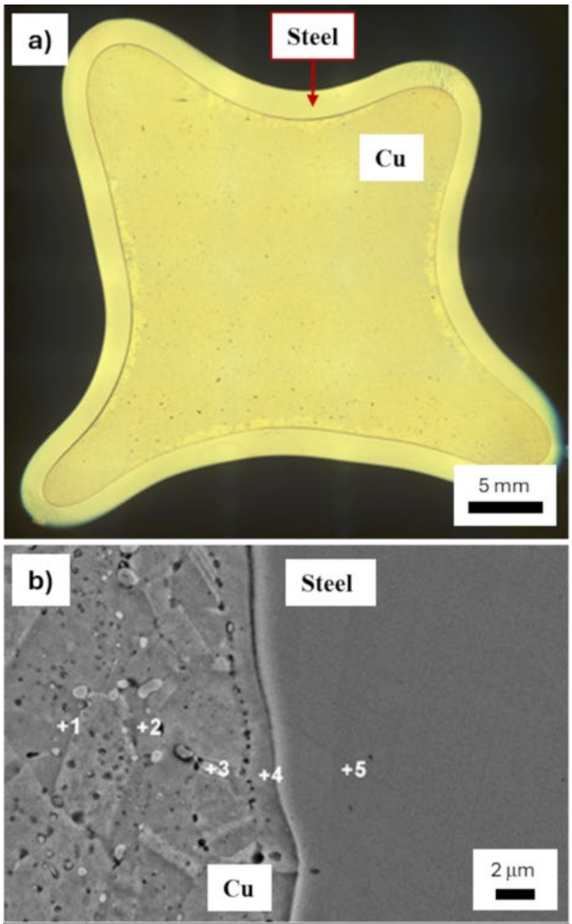

Point	wt, %					
	Cu	Fe	O	Cr	Mg	Ni
1	98.3	1.7	-	-	-	-
2	97.9	2.1	-	-	-	-
3	58.3	1.4	19.2	21.1	-	-
4	96.5	2.8	-	0.7	-	-
5	-	74.0	-	18.0	1.1	6.9

Fig. 8. Microstructure of Cu sinters, process no. 1, a) Cu sinter with steel capsule, b) point chemical composition of Cu-capsule (steel) boundary

Figure 9 displays a cross-section of a carbonyl iron sinter and a steel capsule. Microstructural analysis indicates the occurrence of diffusion phenomena between the capsule material and the Fe sinter. Chromium diffusion from the steel into the carbonyl iron was observed, encompassing a layer approximately 20 µm thick. Figure 10 presents the microstructure of the carbonyl iron sinter after mechanical removal of the lower part of the capsule. The material structure shows clearly formed grains with an average size of approximately 50 µm. The uniformity of the grain shape suggests stable thermal conditions and no significant interference with the sintering process. Chemical composition analysis (EDS) revealed the presence of oxygen at a level of approximately 1.3% by mass on the surface of the analysed sample.

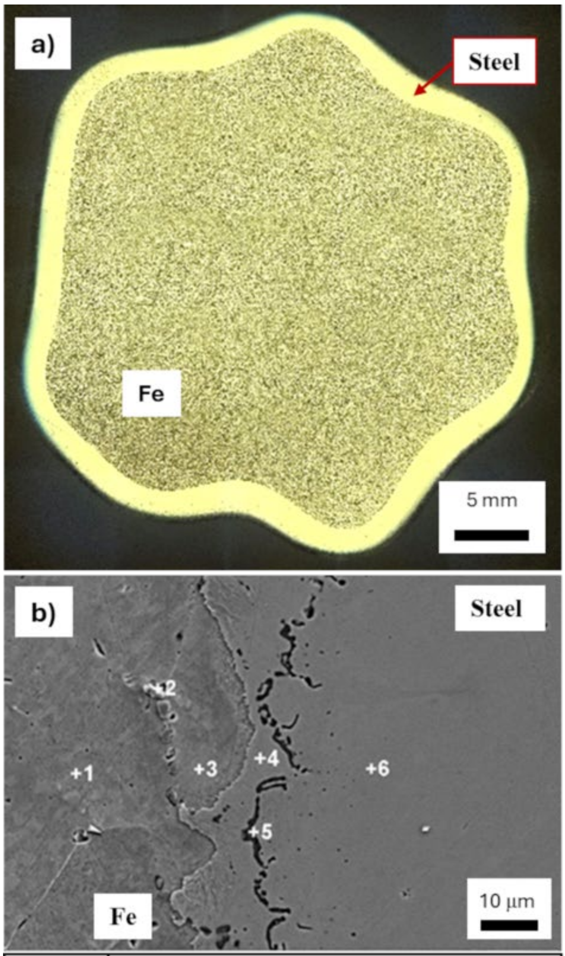

Point	wt, %				
	Fe	O	Cr	Mg	Ni
1	100	-	-	-	-
2	71.7	13.6	14.7	-	-
3	98.1	-	1.9	-	-
4	90.1	-	7.1	0.2	2.6
5	32.8	24.4	28.9	12.9	1.0
6	72.3	-	19.2	1.2	7.3

Fig. 9. Microstructure of carbonyl iron sinter and steel capsule cross-section with EDS analysis at marked points, process no. 2

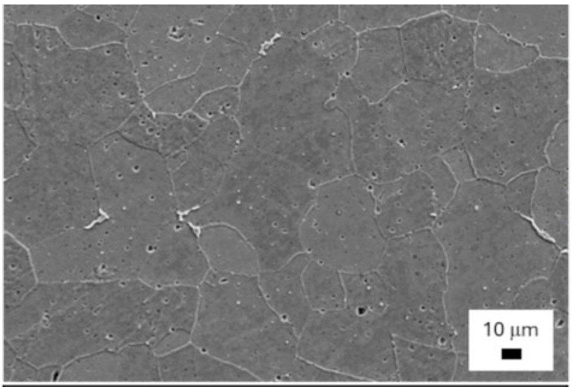

wt, %	
Fe	O
98.7	1.3

Fig. 10. Microstructure of iron sinter along with EDS chemical composition analysis results from sinter surface, process no. 2

Figures 11 and 12 show the microstructure of the Cu(TiN)2 composite obtained using technological process no. 3. Observation of the Cu(TiN)2 sinter–steel capsule interface indicates significant diffusion of the alloying elements, particularly chromium (Cr) and iron (Fe), from the steel capsule into the copper matrix. This phenomenon directly confirms the intensity of diffusion processes occurring at the steel–copper interface under high temperature conditions. Analysis of the cross-sections (Figs. 11a, 11b) revealed that chromium atoms diffuse from the steel layer toward the iron-rich region to a depth of approximately 8 µm. This type of diffusion penetration can result in the formation of transition zones with a modified chemical composition, which in turn affects local mechanical properties such as hardness, wear resistance, and residual stresses in the material interface. The chemical composition analysis performed by energy-dispersive X-ray spectroscopy (EDS) did not reveal the presence of oxygen on the surface of the investigated samples (Fig. 12). Therefore, it can be concluded that the experimental conditions used—such as the protective atmosphere (e.g. inert gas) or a vacuum environment—were effective in preventing oxidation of the composite components. Microstructural analysis of the Cu-TiN composites (Figure 12) reveal local, non-uniform distribution of the TiN particles in the copper matrix, which may result from both limitations in the powder mixture preparation stage and local differences in the degree of material densification during pressing.

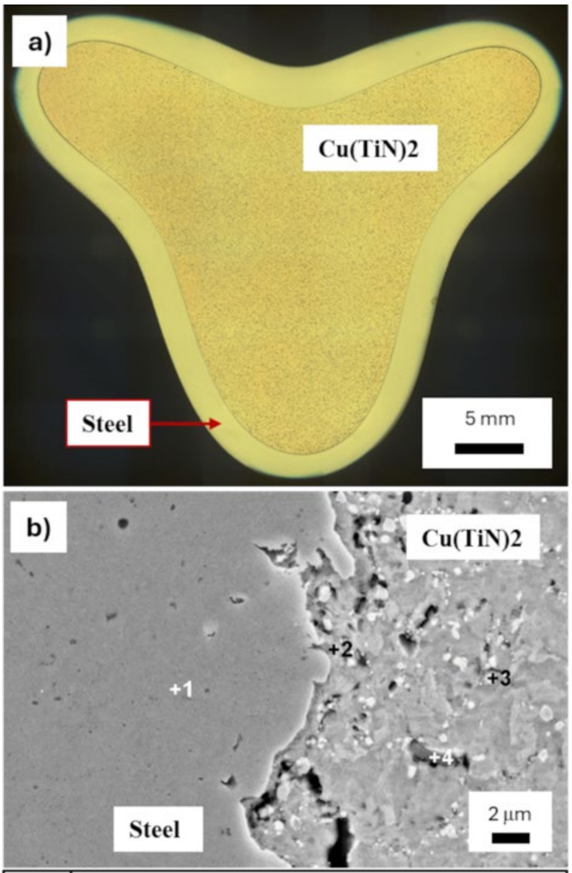

Point	wt, %							
	Fe	Cr	Cu	Ti	O	N	Mg	Ni
1	76.1	15.9	-	0.7	-	-	0.3	7.0
2	4.3	5.5	88.2	0.7	1.3	-	-	-
3	1.7	0.9	97.4	-	-	-	-	-
4	2.3	1.7	40.0	35.2	-	20.8	-	-

Fig. 11. Microstructure of Cu + 2% TiN composite sinter cross-section with EDS analysis at marked points, process no. 3

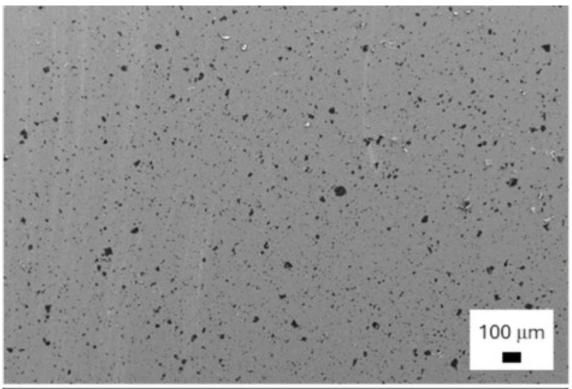

wt, %		
Cu	Ti	N
95.9	4.0	0.1

Fig. 12. Microstructure of Cu + 2% TiN composite sinter with EDS chemical composition analysis results from sinter surface, process no. 3

Examination of the microstructures of the remaining samples did not reveal any significant differences in the microstructure of the Cu-TiN composites.

SUMMARY

Comparative experimental sintering studies of the powders (Cu, Fe and Cu + TiN) demonstrated the beneficial effects of powder encapsulation. Satisfactory results were achieved in terms of porosity (except for process no. 4), as well as hardness and electrical conductivity. Simplified microstructural analyses of the resulting Cu-TiN composites indicate a relatively uniform distribution of titanium nitride within the copper matrix. In the case of copper powder sintering, the diffusion of chromium and iron from the steel capsule into the copper up to a certain depth was observed. The employed encapsulation and HIP sintering process is one of the options for producing composite sintered materials. The method presented in the article allows the production of new composite materials that are difficult or impossible to obtain by other methods. By mixing the powders, then encapsulating and sintering them under pressure, a fully finished material is produced, which, following further processing, can become a finished product.

Various properties of the sinters were obtained as a result of the processes. This is related to the use of different HIP sintering parameters, the bulk density of the powders, the powder compaction technique in the capsule prior to the HIP sintering process, and the design of the steel capsule (the prior stress and deformation state of the material from which it is made).

From previously conducted research [14], it is known how important the form of precipitates/particles formed in copper-based materials is for the structure. Cu-TiN composites with this structure are expected to exhibit both high mechanical strength and good electrical conductivity. The materials obtained in this way will constitute an important basis for further research on the development of modern nanocrystalline materials characterised by a combination of high mechanical properties and electrical conductivity.

CONCLUSIONS

Based on the experimental studies, it can be concluded that:

- Using the Cu + TiN powder encapsulation method in the HIP process enables the production of high-density sinters, good chemical homogeneity, and the potential for further working into products with desired properties.
- Adding TiN to copper increased the sinter hardness from 37 HBW (Cu) to 44 (2% TiN) to 52 (4% TiN), with a simultaneous slight decrease in electrical conductivity from 56 MS/m (Cu) to 52-48 MS/m, respectively.

Funding

The research leading to these results was conducted under a subsidy funded from own funds entitled "Opracowanie technologii wytwarzania materiałów metalicznych przy zastosowaniu urządzenia do puszkowania materiałów proszkowych przeznaczonych do spiekania w procesie HIP", Report no. 8621/G/2025.

REFERENCES

[1] M.A. Meyers, A. Mishra, D. . Benson, Mechanical properties of nanocrystalline materials, Progress in Materials Science, 51, (2006) 427–556, DOI:10.1016/j.pmatsci.2005.08.003

[2] Islam, Zoheir N. Farhat, The influence of porosity and hot isostatic pressing treatment on wear characteristics of cast and P/M aluminium alloys Wear 271 (2011) 1594–1601, https://doi.org/10.1016/j.wear.2011.01.037

[3] HIP-Today-and-Tomorrow.pdf, Franz X. Zimmerman, Jerry Toops, Hot Isostatic Pressing: Today and Tomorrow January (2008) [access: 08.04.2026 r.], http://hasmak.com.tr/tozpdf/

[4] Animesh Bose, William B. Eisen, Hot Consolidation of Powders & Particulates, Metal Powder Industries Federation, 2003, USA

[5] V. Atkinson, S. Davies, Fundamental aspects of hot isostatic pressing: An overview, Metallurgical and Materials Transactions A, 31A, (2000) pages 2981–3000, https://doi.org/10.1007/s11661-000-0078-2

[6] M.H. Bocanegra-Bernal, Hot Isostatic Pressing (HIP) technology and its applications to metals and ceramics, Journal of Materials Science, 39 (2004) 6399-6420, https://link.springer.com/article/10.1023/B:JMSC.0000044878.11441.90

[7] B. Jóźwik, A. Radoń, S. Topolska, J. Kalabis, M. Karpiński, W Burian, D. Kołacz, M. Polak, A. Brudny, W. Łoński, A. Kolano-Burian, Influence of SLM printing parameters and hot isostatic pressure treatment on the structure and properties of CuNi3Si1 alloy, Journal of Alloys and Compounds 947 June (2023) 169531, https://doi.org/10.1016/j.jallcom.2023.169531

[8] D. Kołacz, J. Kulasa, K. Krukowski, A. Hury, G. Muzia, M. Osadnik, J. Kalabis, Effect of sintering temperature and isostatic pressure on selected properties of selected electrical contact materials manufactured by hot isostatic pressing, Composites Theory and Practice 2 (2023) 67-75, https://doi.org/10.62753/ctp.2023.01.2.2

[9] Introduction to Hot Isostatic Pressing Technology, A Guide for Designers and Engineers, EPMA, https://www.publications.epma.com/product/introduction-to-hot-isostatic-pressing-technology/ [access: 08.04.2026 r.].

[10] https://www.bsbf2024.org/wp-content/uploads/2024/10/BSBF24_CoorsTek.pdf [access: 13.04.2026].

[11] J. Wang, S. Srivatsa, Z. Wu, Z. Huang, Modeling of Metal Powder Densification under Hot Isostatic Pressing, Materials 17, 1933, (2024), https://doi.org/10.3390/ma17081933

[12] R. Ni, P. Zhang, L. Che, Z. Lv, S. Chen, W. Qi, L. Zhang, X. Li, Research on improving the simulation accuracy of HIP near-net-shape forming by coupling DEM and FEM Journal of Materials Research and Technology, 36, May–June 2025, 949–962, https://doi.org/10.1016/j.jmrt.2025.03.130

[13] Włodzimierz Bochniak, Andrzej Korbel, Paweł Ostachowski, Marek Łagoda, Plastic flow of metals under cyclic change of deformation path conditions, Archives of Civil and Mechanical Engineering, 3, 2018, 679–686, https://doi.org/10.1016/j.acme.2017.11.004

[14] Z. Rdzawski, J. Stobrawa, W. Głuchowski, J. Sobota, Mechanism and Kinetics of precipitation process in selected copper alloys; Archives of Metallurgy and Materials 59, 2, 649–658, https://doi.org/10.2478/amm-2014–0106

